Production of fuel-cell grade H_2 by sorption enhanced steam reforming of acetic acid as a model compound of biomass-derived bio-oil

María V. Gil[a,b], Javier Fermoso[c], Covadonga Pevida[a], De Chen[b], Fernando Rubiera[a,*]

[a] Instituto Nacional del Carbón, INCAR-CSIC, Apartado 73, 33080 Oviedo, Spain

[b] Department of Chemical Engineering, Norwegian University of Science and Technology, Sem Sælands vei 4, Trondheim, NO-7491, Norway

[c] IMDEA Energy Institute, Thermochemical Processes Unit, Avenida Ramón de la Sagra 3, 28935 Móstoles, Spain

Abstract

Fuel-cell grade H_2 has been produced by the sorption enhanced steam reforming (SESR) of acetic acid, a model compound of the bio-oil obtained from the fast pyrolysis of biomass. A Pd/Ni-Co catalyst derived from a hydrotalcite-like material (HT) with dolomite as CO_2 sorbent was used in the process. A fixed-bed reactor with three temperature zones was employed to favor the catalytic steam reforming reaction in the high-temperature segment, the SESR reaction in the intermediate-temperature part, as well as the water-gas shift (WGS) and CO_2 capture reactions in the low-temperature segment. Different conditions of pressure, temperature, steam/C molar ratio and weight hourly space velocity (WHSV) in the feed were evaluated. Higher steam/C molar ratios and lower WHSV values facilitated the production of H_2 and reduced the concentrations of CH_4, CO and CO_2 in the produced gas. A fuel-cell grade H_2 stream with a H_2 purity of 99.8 vol.% and H_2 yield of 86.7% was produced at atmospheric pressure, with a steam/C ratio of 3, a WHSV of 0.893 h^{-1} and a temperature of 575 ºC in the intermediate part of the reactor (675 ºC in the upper segment and 425 ºC in the bottom part). At high pressure conditions (15 atm) a maximum H_2 concentration of 98.31 vol.% with a H_2 yield of 79.81% was obtained at 725 ºC in the intermediate segment of the reactor (825 ºC in the upper segment and 575 ºC in the bottom part). Under these conditions an effluent stream with a CO concentration below 10 ppm (detection limit)

* Corresponding author. Tel.: +34 985119090; fax: +34 985297662.

E-mail address: frubiera@incar.csic.es (F. Rubiera).

was obtained at both low and high pressure, making it suitable for direct use in fuel cell applications.

Keywords: Hydrogen; Fuel cell; Bio-oil; Sorption enhanced steam reforming (SESR); Pd/Ni-Co catalyst

1. Introduction

The worldwide demand for hydrogen for both chemical and energy uses is expected to increase in the medium-to-long term. Hydrogen is a clean fuel and energy carrier that, coupled with a fuel cell, has the potential to provide clean electricity due to the fact that both the fuel efficiency and level of CO_2 emissions of fuel cell-based systems are greatly improved compared to conventional power sources [1]. The most widespread and established technology for hydrogen production on a commercial scale nowadays is still the steam methane reforming (SMR) of natural gas. This reaction is performed at high temperature and high pressure, is strongly endothermic and produces CO_2. The process incorporates a high temperature catalytic SMR reactor (800-900 ºC; 15-30 bar), one or two catalytic water-gas shift (WGS) reactors (200-400 ºC) and a pressure swing adsorption (PSA) unit, since the product gas is usually fed to a PSA unit in order to obtain a high-purity (>99.9 vol.%) stream of H_2. Hence, besides the consumption of fossil fuels, the overall process entails high capital costs [2]. This explains the increasing interest in the development of more energy-efficient and cost-competitive technologies for the production of hydrogen from renewable sources, such as biomass.

To overcome the disadvantages of SMR, the sorption enhanced steam reforming (SESR) process has received a great deal of attention in recent years. During the SESR process the steam reforming (SR), WGS and CO_2 capture reactions can be conducted simultaneously in one single reactor in conditions of moderate temperature and pressure. The CO_2 is removed in-situ by a sorbent as it is formed and hence the production of H_2 is favored due to the shift of the reaction equilibrium towards hydrogen production. Different configurations of fixed or fluidized bed reactors have been proposed for carrying out the process. Basically the reactor is packed with a mixture of a reforming catalyst and a CO_2 chemisorbent, while the feed gas (fuel +

steam) is passed through the bed [3]. The CO_2 by-product is removed from the reaction zone by the sorbent and a stream of pure H_2 is produced at feed gas pressure. The sorbent needs to be periodically regenerated to allow a cyclic operation. The most commonly used sorbents are CaO-based, since they can repeatedly capture CO_2 via consecutive CaO-carbonation and $CaCO_3$-calcination cycles as indicated by Eq. (1):

$$CaO_{(s)} + CO_{2(g)} \leftrightarrow CaCO_{3(s)} \qquad \Delta H_r^0 = -178 \text{ kJ mol}^{-1} \qquad (1)$$

Natural CaO-based sorbents, such as limestone and dolomite, are able to react with CO_2 at low CO_2 partial pressures and moderate temperature, and show fast kinetics and good adsorption capacities. Although these materials usually suffer from decay in CO_2 capture capacity after several carbonation/calcination cycles [4], they are preferably used in SESR studies due to their wide availability and very low cost [5-8].

Acetic acid is the fuel selected for the study of the SESR process in the present work, as it is one of the most representative constituents of the water soluble fraction of bio-oils produced from the fast pyrolysis of biomass, and hence is frequently used as a model compound of bio-oil in literature [9-13]. Since the bio-oil is derived from biomass resources, the catalytic steam reforming of bio-oil constitutes a renewable energy conversion method for producing hydrogen. Fast pyrolysis involves lower temperatures and shorter reaction times than gasification and produces mostly a liquid fraction. Bio-oil could be used for indirect cofiring in conventional power plants, direct decentralized heating purposes, and potentially as a high energy-density intermediate material suitable for long-distance transportation to destinations where it can be finally converted into chemicals and/or fuels. The use of bio-oil in the SESR process is advantageous because it has a higher energy density and it is easier to transport than raw biomass.

The overall reaction for the conversion of acetic acid to hydrogen, which is a combination of steam reforming and WGS reactions, is expressed by Eq. (2) as follows:

$$C_2H_4O_2 + 2H_2O \rightarrow 4H_2 + 2CO_2 \qquad \Delta H_r^0 = +184 \text{ kJ mol}^{-1} \qquad (2)$$

According to this reaction, 4 mol of hydrogen gas can theoretically be produced from the steam reforming of one mol of acetic acid. However, due to thermodynamic equilibrium limitations and complex reaction pathways, side reactions such as thermal decomposition or methanation usually occur, leading to the formation of intermediates and coke. Thus, the main products of the reforming process include H_2, CO_2, CH_4 and

CO. In the sorption enhanced H_2 production process, the sorbent removes the CO_2 from the gas phase as it is formed, promoting the direct WGS and reforming reactions due to an equilibrium shift effect. As a result, the CO and CH_4 contents are significantly reduced while the H_2 concentration and conversion are increased. Production of hydrogen with low levels of CO, CO_2 and CH_4 is critical for the generation of energy by means of hydrogen fuel cells [14]. The resulting reaction for the SESR process of acetic acid is represented in Eq. (3):

$$C_2H_4O_2 + 2H_2O + 2CaO_{(s)} \rightarrow 4H_2 + 2CaCO_{3(s)} \qquad \Delta H_r^0 = -172 \text{ kJ mol}^{-1} \qquad (3)$$

It can be seen that the SESR process with CaO as CO_2 sorbent is exothermic and no additional energy is required in the reforming stage.

However, a very active catalyst must be used to obtain a high yield of very pure hydrogen from SESR for fuel-cell applications, since the temperatures used in this process are relatively low (400-650 ºC). Furthermore, the catalyst must be stable, since it goes through multiple oxidation/reduction cycles, corresponding to the calcination/carbonation stages [15]. In the present work, a Pd/Ni-Co catalyst has been synthesized and employed, since in a previous study it was demonstrated to be a promising material for use in the SESR process [16]. It shows a good reforming performance and allows the cycling operation of the sorption enhanced reforming process. Additionally, the Pd/Ni-Co catalyst makes the catalyst reduction step between the air-regeneration and reforming stages unnecessary due to the ability of Pd to promote the rapid production of H_2 and hence facilitate an early reduction of the metal oxide phases in the catalyst.

The SESR process has been shown to improve the hydrogen production compared to conventional SR and satisfactory results have been reported in the literature after the SESR of methane [17-21]. Values of H_2 purity as high as 94 vol.% have been obtained at atmospheric pressure, 650 ºC and at a steam/C ratio of 3.2 using a $NiO/NiAl_2O_4$ catalyst and a CaO-based synthetic sorbent, with a CO concentration as low as 2 vol.% [15]. Likewise, a H_2 purity value of 95 vol.% has been reported at 15 atm, 725 ºC and at steam/C ratio of 4 using a NiO/Al_2O_3 catalyst and CaO as sorbent [22]. The benefits of the SESR of biomass compounds compared to SR have also been demonstrated with pyrolysis oils obtained from bunches of palm fruit and pine [23] or waste cooking oil [24]. Other experimental results from the SESR of biomass-derived compounds have

been reported in the literature using mixtures of different Ni-Co HT catalysts and calcined dolomite as CO_2 acceptor. These studies were carried out at atmospheric pressure, temperatures between 550-650 ºC, and at steam/C molar ratios of 3-9. Thus, high-purity H_2 (96.1-99.9 vol.%) with a low CO content (0.012-1.4 vol.%) was obtained from the SESR of bio-syngas from gasified biomass [25], bio-ethanol [26], lignocellulosic biomass [27], sugars from hydrolyzed biomass [28], pure glycerol [2, 29] and crude glycerol, a by-product of biodiesel production [30]. However, the level of CO in the hydrogen stream obtained in these studies is too high for direct use in fuel cells. To produce very pure hydrogen directly from biomass in a single step is still a formidable challenge.

Low temperature proton exchange membrane (PEM) fuel cells require very low CO levels (<10 ppm) in a H_2-rich gas stream in order to be able to suppress the poisoning effect of CO on the PEM fuel cell catalysts [31,32]. The production of very pure hydrogen is therefore an important step for overcoming the CO poisoning problem. The WGS reaction is usually used in fuel processing for fuel cell applications with the purpose of reducing the level of CO. It is often followed by a preferential oxidation (PrOx) step for a final clean-up, where most of the residual CO is oxidized to CO_2. SESR could be an appropriate one-step high-purity hydrogen production process, which would greatly simplify the procedure, increase energy efficiency and reduce costs [33].

The objective of the present paper is to produce fuel cell-grade hydrogen in a single process, which has not been previously reported in the literature. To achieve this objective, the SESR of acetic acid, as a bio-oil model compound, using a Pd/Ni-Co catalyst and dolomite as CO_2 sorbent was performed in a fixed bed reactor. Three zones of descending temperature were employed along the length of the reactor in order to be able to produce a high-purity H_2 stream suitable for direct use in low-temperature PEM fuel cells. Thus, the proposed process involves favoring the catalytic reforming reaction in the high-temperature upper segment, the SESR reaction in the intermediate-temperature part, and the WGS and CO_2 capture reactions in the low-temperature bottom segment. The influence of the operating parameters (pressure, temperature, steam/C molar ratio and space velocity) on the SESR of acetic acid was studied. The experimental results were compared with the equilibrium predictions obtained by means of the Aspen Plus process simulator under identical conditions to the experimental ones.

2. Experimental

2.1. Fuel

Acetic acid was selected as an oxygenated model compound of the organic acids present in the aqueous phase of bio-oils produced by the fast pyrolysis of biomass. Glacial acetic acid was supplied by PANREAC (100% purity). Aqueous solutions of acetic acid were prepared using water-to-acetic acid molar ratios of 2, 4 and 6 (steam/C molar ratios of 1, 2 and 3).

2.2. CO_2 sorbent

Arctic dolomite, used as a precursor of CaO for the capture of CO_2, was supplied by Franefoss Miljøkalk As, Norway. It has a purity of 98.5 wt.% $CaMg(CO_3)_2$ and does not contain any sulfur according to X-ray fluorescence analysis. The dolomite sample was calcined in an air flow (200 mL min^{-1}) at 770 ºC for 4 h prior to its use as CO_2 sorbent. Its initial maximum CO_2 capture capacity was estimated as being 0.46 g CO_2/g sorbent. The dolomite was ground and sieved to reach a particle size of 125-250 μm. The BET surface area and pore volume of the calcined dolomite are 11.0 m^2 g^{-1} and 0.16 cm^3 g^{-1}, respectively, while its average pore size is 59 nm [16].

2.3. Catalyst preparation

The 1%Pd/20%Ni-20%Co HT catalyst (Pd/Ni-Co HT) was prepared by the incipient wetness impregnation method using a 20%Ni-20%Co hydrotalcite-like material (Ni-Co HT) as precursor. The Ni-Co HT precursor was prepared by co-precipitation according to the method reported by He et al. [34] and it was impregnated with a 1% (w/w) load of Pd. The Pd solution was prepared by dissolving $PdCl_2$ into two equivalents of HCl and diluting them in ethanol to the desired concentration. The sample was dried and calcined in an air flow at 500 ºC for 1 h in a muffle oven. The calcined catalyst was pelletized, ground and sieved to the desired particle size (125-250 μm). It was then reduced at 670 ºC for 10 h in a mixed flow (100 cm^3 min^{-1}) of 50 vol.% of H_2 (balance N_2). Finally, the catalyst was passivated by flowing 0.5 vol.% of O_2 in a N_2 stream for 1.5 h and then stored. A detailed description of the Pd/Ni-Co HT catalyst preparation procedure and characterization has been reported elsewhere [16, 27].

Briefly, the Pd/Ni-Co HT catalyst has a BET surface area of 144 m^2 g^{-1}. Its average pore size of 12 nm suggests that the catalyst is a mesoporous material. The metal dispersion estimated by chemisorption of H_2 on the reduced catalyst is 7.8%, while the particle size and the metal surface area are 13 nm and 21 m_{metal}^2 $g_{catalyst}^{-1}$, respectively.

2.4. Sorption enhanced steam reforming (SESR) experiments

A schematic diagram of the experimental setup used for the catalytic SESR experiments with acetic acid is shown in Fig. 1a. It consists of a purpose-built downdraft fixed bed stainless steel reactor (with an internal diameter of 13 mm and a height of 305 mm). The reactor is located inside a tubular electric furnace equipped with three temperature zones: an upper segment at the highest temperature, an intermediate part at the intermediate temperature and a lower part at the lowest temperature. The reaction temperatures are measured by K-type thermocouples which are inserted into the catalyst/sorbent bed. The pressure is measured by a pressure transducer and automatically controlled by a micro-valve. The gas flow rates are controlled by Bronkhorst® mass flow controllers, while the aqueous solution of acetic acid is fed in by means of a Gilson® high-performance liquid chromatography (HPLC) pump.

The reactor was loaded with a 18 g mixture of calcined dolomite (as CO_2 sorbent) and Pd/Ni-Co catalyst, at a sorbent-to-catalyst ratio of 8 g/g. SESR experiments were carried out at 1 and 15 atm and isothermally at temperatures between 525 and 775 ºC in the intermediate segment of the reactor (40 mm). This intermediate temperature will be referred as 'experiment temperature' from now on, while the terms 'high-temperature' and 'low-temperature' will be used to refer to the temperature in the upper (80 mm) and lower (30 mm) segments of the reactor, respectively. The low-temperature is 150 ºC lower than the experiment temperature, while the high-temperature is 100 ºC higher than the experiment temperature. The temperature profile in the reactor and the location of the thermocouples is shown in Fig. 1b.

Prior to each SESR experiment, the catalyst/sorbent mixture was subjected to a regeneration step at 770 ºC and at 1 atm (or 925 ºC and 15 atm in the case of the high-pressure experiments) in an air flow (200 NmL min^{-1}) until the CO_2 level fell to less than 0.1 vol.%. The regeneration temperatures were selected taking into consideration the thermodynamic limitations of the decarbonation reaction and the kinetics of the

decarbonation of dolomite [26]. Therefore, a regenerated catalyst/sorbent mixture was used in all the SESR experiments in the present study. After regeneration, the reactor was purged with N_2 and cooled down to the desired experimental reaction temperature. Once the operating temperature was reached under a N_2 atmosphere, the acetic acid aqueous solution, swept by a 50 NmL min^{-1} flow of N_2, was evaporated and then pumped downdraft through the catalyst/sorbent bed at different space velocities. The SESR of acetic acid, characterized by an enhanced production of hydrogen due to the removal of CO_2 in situ by the sorbent (prebreakthrough stage), proceeded until the CO_2 sorbent became saturated and lost its capacity for the removal of CO_2 (breakthrough stage). Afterwards, CO_2 capture was negligible (postbreakthrough stage) and a conventional SR process was assumed to take over.

The effluent gas exiting the reactor was directed into a thermoelectric cooler (2-4 ºC) to condense excess steam, unreacted acetic acid and any other liquid that may have formed. The composition of the dry gas was analyzed on-line by a dual channel Varian® CP-4900 Micro GC equipped with a molecular sieve (Molsieve 5 Å) column, a HayeSep A column and a thermal conductivity detector (TCD). Helium was used as the carrier gas. The Micro GC was calibrated employing a standard gas mixture at periodical intervals and the detection limit of the equipment for gas analysis is 0.001 vol.%. The species detected were H_2, CH_4, CO, and CO_2. Their concentrations in the gas product were calculated on the basis of the dry composition of the gas effluent. The flow rates of the species generated during the experiment were calculated by means of a nitrogen balance, on the basis of the amount of nitrogen fed in and the composition of the nitrogen evolved.

The H_2 yield, H_2 selectivity and the concentration of the gas components were calculated from Eq. (4)-(6), respectively:

$$H_2 \text{ yield } (\%) = 100 \cdot (F_{H2}/4 \cdot F_{\text{acetic acid}}) \quad (4)$$

$$H_2 \text{ selectivity } (\%) = 100 \cdot [2 \cdot y_{H2}/(2 \cdot y_{H2} + 4 \cdot y_{CH4})] \quad (5)$$

$$i \text{ (vol.\%)} = 100 \cdot (y_i/\Sigma\, y_i) \qquad (i = H_2, CH_4, CO, CO_2) \quad (6)$$

where F_{H2} is the molar flow rate of the H_2 produced (mol min^{-1}), $F_{\text{acetic acid}}$ is the molar flow rate of the acetic acid fed in (mol min^{-1}), and y_i is the molar content (N_2 free and on a dry basis) of each species i (H_2, CH_4, CO and CO_2). The weight hourly space velocity (WHSV) is defined as the ratio of the mass flow rate of the inlet acetic acid to the mass

of catalyst ($g_{acetic\ acid}\ g_{catalyst}^{-1}\ h^{-1}$).

2.5. Thermodynamic equilibrium calculations

A thermodynamic analysis of the SESR process was conducted at the three temperatures employed in the reactor (high-temperature, experiment temperature and low-temperature) under each one of the experimental reaction conditions studied. Aspen Plus 7.2 software (Aspentech) was used for the calculations. Equilibrium compositions were estimated by minimizing the Gibbs free energy, since this no-stoichiometric approach offers greater flexibility when tackling complex problems where the reaction pathways are unclear. A stoichiometric approach would require a clearly defined reaction mechanism incorporating all chemical reactions and species involved. The non-stoichiometric chemical equilibrium calculation method is incorporated in Aspen Plus as a RGibbs unit operation, which was chosen as the reaction system. RGibbs reactor block uses the criteria of minimization of the Gibbs free energy for all species in the system under phase and chemical equilibria without specification of the possible reactions. The Peng-Robinson property method was used to predict the thermodynamic behavior of the system. This calculation requires identification of the possible products. According to the results obtained for the prediction of the equilibrium under sorption enhanced and steam reforming conditions, the species produced in concentrations higher than 10^{-4} mol% were H_2, CO, CO_2, CH_4, H_2O, CaO and $CaCO_3$. C_2H_4 and C_2H_6 were also included in the product pool, but their concentrations in the equilibrium stream were either null or not high enough to be considered significant products. The product mole fractions were calculated on a dry basis to compare with experimental results.

3. Results and discussion

3.1. Effect of the temperature and pressure

3.1.1. Thermodynamic equilibrium results

The thermodynamic equilibrium of the SESR process was analyzed at 1 and 15 atm and over a temperature range of 400-900 ºC. Figs. 2-5 show the equilibrium values by means of lines corresponding to three temperatures: high-temperature corresponding to the upper segment of the reactor (‘equilibrium high-T’ lines), experiment temperature

corresponding to the medium part of the reactor ('equilibrium' lines) and low-temperature corresponding to the lower part of the reactor ('equilibrium low-T' lines). The experiment temperature is the one shown on the X-axis. The points represent the experimental results.

In the case of the SESR process (Figs. 2 and 3), the experimental H_2 concentration values (Fig. 2c) are higher, whereas the CO (Fig. 3a) and CO_2 (Fig. 3b) concentrations are much lower, than those of the equilibrium corresponding to both the high-temperature and the experiment temperature. However, they all follow the lines of the equilibrium corresponding to the low-temperature quite closely between 525 and 675 ºC in the case of the experiments at 1 atm and between 675 and 775 ºC for the experiments at 15 atm. At atmospheric pressure and 725 ºC, the H_2 concentration value is below, while the CO and CO_2 concentration values are above, the 'equilibrium low-T' curve.

At atmospheric pressure the equilibrium values for CH_4 (Fig. 3c) in the temperature range studied are low and very similar for all the temperatures studied, although they decrease slightly as the temperature increases. The experimental CH_4 concentrations increase slightly between 525 and 675 ºC at 1 atm, but they are all between the limits of the high-T and low-T equilibrium curves, as also occurs for the experimental H_2 selectivity values (Fig. 2b). At atmospheric pressure and 725 ºC, the CH_4 concentration is above, while the H_2 selectivity is below, the equilibrium curves. At high-pressure, the CH_4 concentrations and the H_2 selectivity values are between the equilibrium values corresponding to the high-temperature and low-temperature.

Finally, the experimental H_2 yield values (Fig. 2a) are below the 'equilibrium high-T' curve between 525 and 625 ºC at atmospheric pressure and between 675 and 775 ºC at 15 atm, although this equilibrium is almost reached at the highest temperature. The values for the SESR experiments at atmospheric pressure and between 675 and 725 ºC are between the 'equilibrium high-T' curve and that of the equilibrium corresponding to the experiment temperature. Therefore, the H_2 yield values are far away from those corresponding to the 'equilibrium low-T' curve for all the experimental conditions analyzed.

These results indicate that when the gas effluent crosses the bed in the lower part of the reactor (at the lowest temperature), CO_2 capture increases and CO is converted by WGS, and so CO_2 and CO concentrations decrease to values corresponding to the

equilibrium at the lowest temperature ('equilibrium low-T' curve). Both the WGS reaction and the steam reforming reaction are enhanced by the capture of CO_2, which leads to an increase in H_2 concentration, helping to reach the equilibrium value corresponding to the low-temperature.

In general, similar trends regarding to the equilibrium were obtained in the case of the SR process (Figs. 4 and 5) than those for the SESR process. The experimental CO (Fig. 5a), CO_2 (Fig. 5b) and CH_4 (Fig. 5c) concentrations follow the 'equilibrium low-T' curve quite accurately, or they are close, for the experiments at both 1 and 15 atm. These results indicate that the lower temperature maintained during the experiments in the lower part of the reactor clearly favors the conversion of CO via the WGS reaction during the SR process. For the H_2 yield (Fig. 4a), H_2 selectivity (Fig. 4b) and H_2 concentration (Fig. 4c), their values are higher than those of the 'equilibrium low-T' curve at the lower temperatures studied, but slightly lower in the higher temperature range. Therefore, the SR results indicate that the SR reaction occurred in the upper part of the reactor where the temperature was high enough, but it is probable that the H_2 equilibrium concentrations corresponding to that temperature were not reached. This seems to be confirmed by the fact that the CH_4 concentrations are above the values corresponding to the equilibrium at the highest temperature. However, as the temperature was reduced in the lower part of the reactor, the WGS was favored and the consumption of CO promoted, which can be deduced from the experimental CO concentrations that are similar to those of the low-temperature equilibrium. This implies an increase in the H_2 concentration, H_2 selectivity and H_2 yield, which are higher than those of the low-T equilibrium.

Therefore, for both SESR and SR the comparison between the equilibrium and experimental results suggests that the effluent composition is determined by the temperature at the reactor outlet. Thermodynamic equilibrium results show that the low temperature at the lower segment of the reactor favors the WGS reaction and hence the hydrogen purity, which demonstrates the advantages of the purposed strategy for the production of highly pure hydrogen by using three-temperature zones in the reactor.

3.1.2. Experimental results of the SESR process

Figs. 2 and 3 show the experimental results as a function of the experiment temperature during the SESR process. The H_2 yield (Fig. 2a) increases with the temperature up to 86.7% (at 575 ºC and atmospheric pressure) and 79.8% (at 725 ºC and 15 atm), evidencing a slight decrease at higher temperatures. The H_2 selectivity (Fig. 2b) shows very high values (>99.6%) at temperatures between 525-675 ºC at atmospheric pressure and it decreases at 725 ºC (97.1%). However, at 15 atm the H_2 selectivity values are very similar for the range of temperatures studied (around 97.2%).

At atmospheric pressure the H_2 concentration (Fig. 2c) reaches values as high as 99.8 vol.% at 525 and 575 ºC, and 99.6 vol.% at 625 and 675 ºC. Further increase in the experiment temperature up to 725 ºC leads to a significant reduction in the H_2 purity (95.0 vol.%). However, similar concentrations of H_2 are obtained when SESR is carried out at 15 atm (98.3 vol.%) irrespective of the temperature. The different trends with temperature for the H_2 yield and H_2 concentration indicate that a compromise between these parameters must be accepted in order to establish an optimum temperature for the SESR process under the conditions studied.

The CO concentration (Fig. 3a) is below the detection limit when the temperature is between 525-625 ºC at 1 atm, while a low concentration is observed at 675 ºC (0.02 vol.%). However, a significant value of the CO concentration (0.38 vol.%) is detected at 725 ºC. At 15 atm, CO concentration is below the detection limit when the reaction occurs at 675 and 725 ºC, while only a low CO concentration (0.01 vol.%) is apparent at 775 ºC at high pressure. The favorable thermodynamics of the WGS reaction (exothermic) at low temperature explains the lower CO concentrations found at the lowest temperatures studied.

At atmospheric pressure, the CO_2 concentration (Fig. 3b) is very low when SESR takes place at 525 and 575 ºC (0.04 vol.%). It increases slightly when the temperature increases up to 675 ºC (0.18 vol.%), but it experiences a greater increase at 725 ºC (3.4 vol.%). For SESR at 15 atm, the CO_2 concentration is below the detection limit at 675 and 725 ºC, while a low concentration value is recorded at 775 ºC (0.13 vol.%). In this case, the favorable thermodynamics of the carbonation reaction (exothermic) at low temperature explains why the CO_2 concentration increases with increasing temperature since high temperatures inhibit the removal of CO_2 to some extent. This means that a

very weak CO_2 sorption occurs when the experiment temperature reaches 725 ºC at atmospheric pressure, resulting in a poor sorption enhancement of the process. Since CO_2 sorption leads to an enhancement in H_2 production by shifting the equilibrium of the steam reforming and WGS reactions to the products side, lower values of H_2 concentration and higher concentrations of CO are also found at the highest temperature studied.

The CH_4 concentration (Fig. 3c) increases slightly (from 0.12 to 0.20 vol.%) as the temperature increases from 525 and 675 ºC at 1 atm, whereas a much higher CH_4 content is detected at 725 ºC (1.25 vol.%). The low CH_4 concentrations below 675 ºC are indicative of the ability of the Pd/Co-Ni HT catalyst to suppress the methanation reaction due to the enhancement of the WGS reaction and/or to the successful catalysis of the methane steam reforming reaction. An approximately constant CH_4 concentration is maintained when the SESR process occurs between 675-775 ºC at 15 atm (1.7 vol.%). In general, these results are in good agreement with those obtained for the SESR of other biomass fuels, such as ethanol [26] or sorbitol and glucose [28].

In summary, the results indicate that an increase in the temperature above 675 ºC during the SESR of acetic acid at atmospheric pressure significantly decreases the H_2 yield, H_2 selectivity and H_2 concentration, while simultaneously increases the CH_4, CO and CO_2 concentrations. On the other hand, no significant differences are detected in the results when the SESR process of acetic acid is performed at 15 atm between 675-775 ºC. However, if a fuel-cell grade stream of H_2 (i.e., CO concentration <10 ppm) is required, the SESR of acetic acid should be performed between 525-625 ºC in the intermediate segment of the reactor at atmospheric pressure or between 675-725 ºC at 15 atm.

Figs. 2 and 3 also show higher values for the H_2 yield, H_2 selectivity and H_2 concentration, as well as lower values for the CH_4 concentration, when the process is carried out at 675 ºC and at atmospheric pressure compared to the high-pressure conditions (15 atm). Atmospheric pressure is thermodynamically favorable for producing a high concentration of H_2. An increase in the pressure does not favor the production of hydrogen, whereas it promotes the formation of methane by the methanation reaction. Since low pressure is also favorable for the decarbonation reaction of the solid CO_2 acceptor, most sorption enhanced reforming studies have been

performed at atmospheric pressure. However, the production of H_2 at atmospheric pressure might lead to an energy penalty, as compressed H_2 is required for its transportation and storage [35]. However, it should be noted that at 675 ºC low concentrations of CO and CO_2 are produced at atmospheric pressure, whereas these gases are below the detection limit in the effluent at 15 atm. When the experiment temperature is increased up to 725 ºC, the H_2 yield is only slightly higher at 1 atm, whereas the H_2 concentration is much higher at 15 atm due to the very high concentrations of CO and CO_2 present in the effluent at atmospheric pressure. The results indicate that at higher pressures, the temperature needs to be elevated considerably to achieve the same level of H_2 concentration as that obtained at atmospheric pressure. The CO and CO_2 concentrations are still below the detection limit when the process is carried out at 725 ºC and 15 atm. As a result, at high pressures, CH_4 is the dominant impurity in the production of hydrogen.

3.1.3. Experimental results of the SR process

The experimental results corresponding to the SR process are shown in Figs. 4 and 5. It can be observed that the H_2 yield (Fig. 4a), H_2 selectivity (Fig. 4b), H_2 concentration (Fig. 4c) and CO concentration (Fig. 5a) increase as the experiment temperature increases. Also, their values are significantly higher when the reforming process is performed at atmospheric pressure compared to high-pressure conditions. As a result of the endothermic character of the reforming reaction, higher temperatures favor the conversion of fuel and hence lead to a higher concentration of H_2. On the other hand, the CO_2 (Fig. 5b) and CH_4 (Fig. 5c) concentrations decrease with temperature, and their values are lower for the experiments performed at atmospheric pressure than those at 15 atm. The exothermic character of the WGS reaction leads to higher concentrations of CO and lower concentrations of CO_2 at higher temperatures. Finally, the endothermic character of the reforming reaction of CH_4 would explain the lower concentration of this component at higher temperatures.

In the case of the SR process, the difference between the results obtained at atmospheric pressure and 15 atm is much greater than that observed for the SESR process. Moreover, a clear worsening of the results when the process is carried out at higher pressure is evident at all the temperatures.

3.1.4. Optimum conditions for the SESR of acetic acid

In the SESR process, the highest experimental value of H_2 concentration obtained is 99.84 vol.% at a temperature of 525 ºC in the intermediate segment of the reactor. In this case, the H_2 yield value obtained is 84.19% and the CO concentration is below the detection limit. The H_2 yield can be increased up to 86.66% if the temperature in the intermediate segment of the reactor is increased up to 575 ºC. At this temperature the H_2 concentration (99.82 vol.%) do not experience any notable decrease, while the CO concentration is still below the detection limit.

On the other hand, if the SESR process is to be carried out at 15 atm, the most suitable temperature for the intermediate segment of the reactor would be 725 ºC and, under such conditions, the H_2 yield would be 79.81% and the H_2 concentration 98.31 vol.%, whereas the CO concentration is below the detection limit.

The SESR of acetic acid was previously studied in a fluidized bed reactor at atmospheric pressure and at 575 ºC, with a steam/C ratio of 3 and a WHSV of 0.893 h^{-1} [36]. The results obtained were a H_2 yield of 90.18%, a H_2 selectivity of 99.69% and a H_2 concentration of 99.29 vol.%. A CO content of 0.11 vol.% was also detected. Therefore, although a higher H_2 yield than that of the present study was obtained, the H_2 purity was lower and a fuel-cell grade H_2 stream was not achieved due to the high CO concentration. This clearly indicates that an additional last stage of low temperature during the SESR process is effective to reduce the CO content in the effluent gas.

In summary, from the results obtained in the present work it can be deduced that at atmospheric pressure, a temperature of 575 ºC in the intermediate segment of the reactor (675 ºC in the upper segment of the reactor and 425 ºC in the lower part), at a steam/C ratio of 3 with a WHSV of 0.893 h^{-1}, can be considered as the optimum conditions for the SESR of acetic acid using the fixed-bed reactor configuration of the present study in order to be able to achieve a very high H_2 production and to obtain a fuel-cell grade hydrogen stream.

3.2. Effect of weight hourly space velocity (WHSV)

The effect of the space velocity on the SESR and SR processes was evaluated at atmospheric pressure (at 575 ºC) and under 15 atm (at 775 ºC) conditions. WHSV

values of 0.893, 1.339, 1.786 and 2.679 h^{-1} were studied by changing the total inlet flow rate (5, 7.5, 10 and 15 g h^{-1}, respectively), while maintaining a steam/C molar ratio of 3. Fig. 4 shows the results for the SESR process, whereas Fig. 5 shows the results for SR, as a function of the WHSV.

For the SESR, the H_2 yield (Fig. 4a) decreases significantly with the space velocity in the experiments at both atmospheric and high-pressure. At atmospheric pressure, the H_2 selectivity and H_2 concentration (Fig. 4b), as well as the CO, CO_2 (Fig. 4c) and CH_4 (Fig. 4d) concentrations are almost constant in the range of the space velocities studied. Furthermore, the CO concentration is below the detection limit under such conditions. However, when the SESR process is carried out at 15 atm, the H_2 selectivity and H_2 concentration decrease with space velocity, while the CO, CO_2 and CH_4 concentrations increase. A lower fuel conversion might be expected with an increase in WHSV due to the shorter contact time. In the present work, a worse conversion is reflected in the decrease in the H_2 yield with the space velocity at both pressures. However, at atmospheric pressure the H_2 purity and the CO content are not affected by the increase in WHSV up to 2.679 h^{-1}. Fig. 4 shows that the H_2 yield is affected much more by WHSV than H_2 selectivity and H_2 purity. Similar results for the hydrogen yield were found after the sorption enhanced steam reforming of glycerol [30]. This suggests that, together with a decrease in the conversion, the formation of coke may have occurred at higher space velocities.

In the case of the SR process, the H_2 yield (Fig. 5a), H_2 selectivity and H_2 concentration (Fig. 5b) decrease, while the CO, CO_2 (Fig. 5c) and CH_4 (Fig. 5d) concentrations increase, as the space velocity increases in the experiments at both 1 and 15 atm.

3.3. Effect of steam/C molar ratio

The effect of the steam/C molar ratio on the SESR and SR processes was evaluated at 675 ºC and under atmospheric pressure conditions. Steam/C molar ratios of 1, 2 and 3 were studied by varying the inlet flow of acetic acid (3.13, 2.17 and 1.79 g h^{-1}, respectively), which ensured that the total inlet flow rate of aqueous solution would remain the same (5 g h^{-1}). The experimental results are shown in Fig. 6.

For both the SESR (Fig. 6a) and SR (Fig. 6b) processes, the H_2 yield, H_2 selectivity and H_2 concentration increase with the steam/C molar ratio, mainly when the steam/C molar ratio increases from 1 to 2. In the case of the SESR process, when the steam/C molar ratio increases from 2 to 3, the increase in H_2 selectivity (from 98.95 to 99.56%) and H_2 concentration (from 99.31 to 99.62 vol.%) is relatively small, due to thermodynamic limitations. However, a more significant increase is detected in the case of the H_2 yield (from 82.68 to 85.40%) as the steam/C molar ratio increases up to 3, which can be due to the fact that higher steam/C ratios favor the reaction kinetics, lowering the coke formation. In general, for SESR (Fig. 6c) and SR (Fig. 6d) the CH_4, CO and CO_2 concentrations decrease as the steam/C molar ratio increases, but their decrease is again much higher when the steam/C molar ratio increases from 1 to 2. Low steam/C ratio values enhance methanation, whereas they cause a simultaneous decrease in methane steam reforming and WGS reactions [31]. Thus, the CH_4 concentration was reduced from 8.93 to 0.53 vol.% when the steam/C molar ratio increased from 1 to 2. Methane content is a very important factor for hydrogen selectivity in the SESR process. Likewise, at a low steam/C molar ratio, hydrogen purity is strongly influenced by the methane content. A lower hydrogen production at low values of steam/C ratio has been reported after the SESR of glycerol due to the formation of carbonaceous species on the catalyst that caused a decrease in its activity, so increasing the methane content at the expense of hydrogen production [29]. CO_2 and CO concentrations are almost constant when the steam/C molar ratio increases from 2 to 3 in the case of the SESR process, which indicates that the carbonation reaction is proceeding normally at the studied temperature at both steam/C ratio values.

An optimal steam/C molar ratio of 4.5 at atmospheric pressure, a temperature of 560 ºC and a WHSV of 0.893 h^{-1} have been previously reported in the literature [36] as the ideal conditions for the SESR of acetic acid for hydrogen production in a fluidized bed reactor. This steam/C molar ratio is higher than that used in the present work, and consequently a higher H_2 yield (92.0%) was obtained. However, a slightly lower H_2 purity was achieved (99.53 vol.%) with a higher CO content (0.06 vol.%) in the effluent stream, again showing the advantage of adding an additional low-temperature stage to the reforming process.

Steam is often added beyond the stoichiometric limit in the reforming process in order to promote hydrogen production and to prevent coke formation over the surface of the catalyst. The effect of increasing the steam/C molar ratio is especially important for the H_2 yield (Fig. 6), which is significantly enhanced at higher values of steam/C. A higher amount of steam will increase the conversion of tars and intermediate compounds, and hence contribute to the avoidance of carbon deposits formation during the reforming process. In the present work, the experimental results indicate that catalytic activity is maintained when a steam/C molar ratio of 2 is used. H_2 purity can also be maintained at a reasonably high value under such conditions, with low CO and CO_2 concentrations. If a decrease in the H_2 yield were acceptable, a lower steam/C molar ratio could be used to reduce the heat requirements for steam generation and the associated energy penalty.

4. Conclusions

In order to produce a fuel cell-grade H_2 stream in a single step, the sorption enhanced steam reforming of acetic acid, a model compound of bio-oil obtained from biomass fast pyrolysis, was experimentally investigated. The experimental results demonstrate the possibility of obtaining high-purity H_2 after the SESR of acetic acid in a fixed bed reactor with three-temperature zones over a Pd/Ni-Co HT catalyst using calcined dolomite as CO_2 sorbent. The catalyst used proved to be highly active for the one-step production of fuel-cell grade hydrogen (<10 ppm CO) from the SESR of acetic acid. The optimum conditions for the production of hydrogen by the SESR of acetic acid were found to be 1 atm and 575 ºC in the intermediate part of the reactor (675 ºC in the upper segment and 425 ºC in the lower part) at a steam/C molar ratio of 3 and a WHSV value of 0.893 h^{-1}. Thus, a H_2 concentration of 99.82 vol.%, with a H_2 yield of 86.66% and a H_2 selectivity of 99.71%, were achieved. Low CH_4 and CO_2 concentrations (0.14% and 0.04 vol.%, respectively) and a negligible CO content (below detection limit) were also obtained. For high-pressure conditions (15 atm), a maximum H_2 concentration of 98.31 vol.%, with a H_2 yield of 79.81% and a H_2 selectivity value of 97.04%, can be obtained at 725 ºC in the intermediate segment of the reactor (825 ºC in the upper segment and 575 ºC in the bottom part), together with a low CH_4 concentration (1.69 vol.%) and non-detectable levels of CO and CO_2. Such a

low level of CO in the H_2 stream might allow the direct use of the gas product in low-temperature proton exchange membrane fuel cells without the need for subsequent CO removal. From these results it can be concluded that an additional last stage of low temperature during the SESR process would produce a highly pure H_2 stream suitable for direct application in PEM fuel cells.

5. Acknowledgements

This work was carried out with financial support from the Spanish MINECO (Project ENE2014-53515-P), co-financed by the European Regional Development Fund (ERDF) and the Principado de Asturias (PCTI 2013-2017, GRUPIN14-079). The authors thank Franefoss Miljøkalk A/S (Norway) for supplying Arctic dolomite.

References

[1] C. Rioche, S. Kulkarni, F.C. Meunier, J.P. Breen, R. Burch, Appl. Catal. B-Environ. 61 (2005) 130-139.
[2] B. Dou, C. Wang, H. Chen, Y. Song, B. Xie, Int. J. Hydrogen Energy 38 (2013) 11902-11909.
[3] K.B. Lee, M.G. Beaver, H.S. Caram, S. Sircar, Int. J. Hydrogen Energy 33 (2008) 781-790.
[4] J.C. Abanades, Chem. Eng. J. 90 (2002) 303-306.
[5] N. Hildenbrand, J. Readman, I.M. Dahl, R. Blom, Appl. Catal. A-Gen. 303 (2006) 131-137.
[6] A. Lopez Ortiz, D.P. Harrison, Ind. Eng. Chem. Res. 40 (2001) 5102-5109.
[7] M. Broda, V. Manovic, Q. Imtiaz, A.M. Kierzkowska, E.J. Anthony, C.R. Müller, Environmental Science & Technology 47 (2013) 6007-6014.
[8] Z.-s. Li, N.-s. Cai, J.-b. Yang, Ind. Eng. Chem. Res. 45 (2006) 8788-8793.
[9] J.R. Galdámez, L. García, R. Bilbao, Energy Fuels 19 (2005) 1133-1142.
[10] X. Hu, G. Lu, J. Mol. Catal. A: Chem. 261 (2007) 43-48.
[11] Z. Li, X. Hu, L. Zhang, G. Lu, J. Mol. Catal. A: Chem. 355 (2012) 123-133.
[12] K. Takanabe, K.-i. Aika, K. Seshan, L. Lefferts, Chem. Eng. J. 120 (2006) 133-137.
[13] E.C. Vagia, A.A. Lemonidou, Int. J. Hydrogen Energy 32 (2007) 212-223.
[14] C. Wang, B. Dou, H. Chen, Y. Song, Y. Xu, X. Du, T. Luo, C. Tan, Chem. Eng. J. 220 (2013) 133-142.
[15] A.L. García-Lario, M. Aznar, I. Martinez, G.S. Grasa, R. Murillo, Int. J. Hydrogen Energy 40 (2015) 219-232.
[16] J. Fermoso, M.V. Gil, F. Rubiera, D. Chen, ChemSusChem 7 (2014) 3063-3077.
[17] K.B. Yi, D.P. Harrison, Low-Pressure Sorption-Enhanced Hydrogen Production, Ind. Eng. Chem. Res. 44 (2005) 1665-1669.
[18] K. Johnsen, H.J. Ryu, J.R. Grace, C.J. Lim, Chem. Eng. Sci. 61 (2006) 1195-1202.
[19] C.S. Martavaltzi, A.A. Lemonidou, Chem. Eng. Sci. 65 (2010) 4134-4140.

[20] B. Arstad, R. Blom, E. Bakken, I. Dahl, J.P. Jakobsen, P. Røkke, Energy Procedia 1 (2009) 715-720.
[21] M. Xie, Z. Zhou, Y. Qi, Z. Cheng, W. Yuan, Chem. Eng. J. 207–208 (2012) 142-150.
[22] B. Balasubramanian, A. Lopez Ortiz, S. Kaytakoglu, D.P. Harrison, Chem. Eng. Sci. 54 (1999) 3543-3552.
[23] R.M. Zin, A. Lea-Langton, V. Dupont, M.V. Twigg, Int. J. Hydrogen Energy 37 (2012) 10627-10638.
[24] P. Pimenidou, G. Rickett, V. Dupont, M.V. Twigg, Bioresour. Technol. 101 (2010) 9279-9286.
[25] L. He, D. Chen, ChemSusChem 3 (2010) 1169-1171.
[26] L. He, H. Berntsen, D. Chen, J. Phys. Chem. A 114 (2010) 3834-3844.
[27] J. Fermoso, F. Rubiera, D. Chen, Energy Environ. Sci. 5 (2012) 6358-6367.
[28] L. He, D. Chen, ChemSusChem 5 (2012) 587-595.
[29] L. He, J.M.S. Parra, E.A. Blekkan, D. Chen, Energy Environ. Sci. 3 (2010) 1046-1056.
[30] J. Fermoso, L. He, D. Chen, Int. J. Hydrogen Energy 37 (2012) 14047-14054.
[31] T. Noor, M.V. Gil, D. Chen, Appl. Catal. B-Environ. 150–151 (2014) 585-595.
[32] C.H. Lee, S. Mun, K.B. Lee, J. Power Sources 281 (2015) 158-163.
[33] D.P. Harrison, Ind. Eng. Chem. Res. 47 (2008) 6486-6501.
[34] L. He, H. Berntsen, E. Ochoa-Fernández, J. Walmsley, E. Blekkan, D. Chen, Top. Catal. 52 (2009) 206-217.
[35] D. Chen, L. He, ChemCatChem 3 (2011) 490-511.
[36] M.V. Gil, J. Fermoso, F. Rubiera, D. Chen, Catal. Today 242, Part A (2015) 19-34.

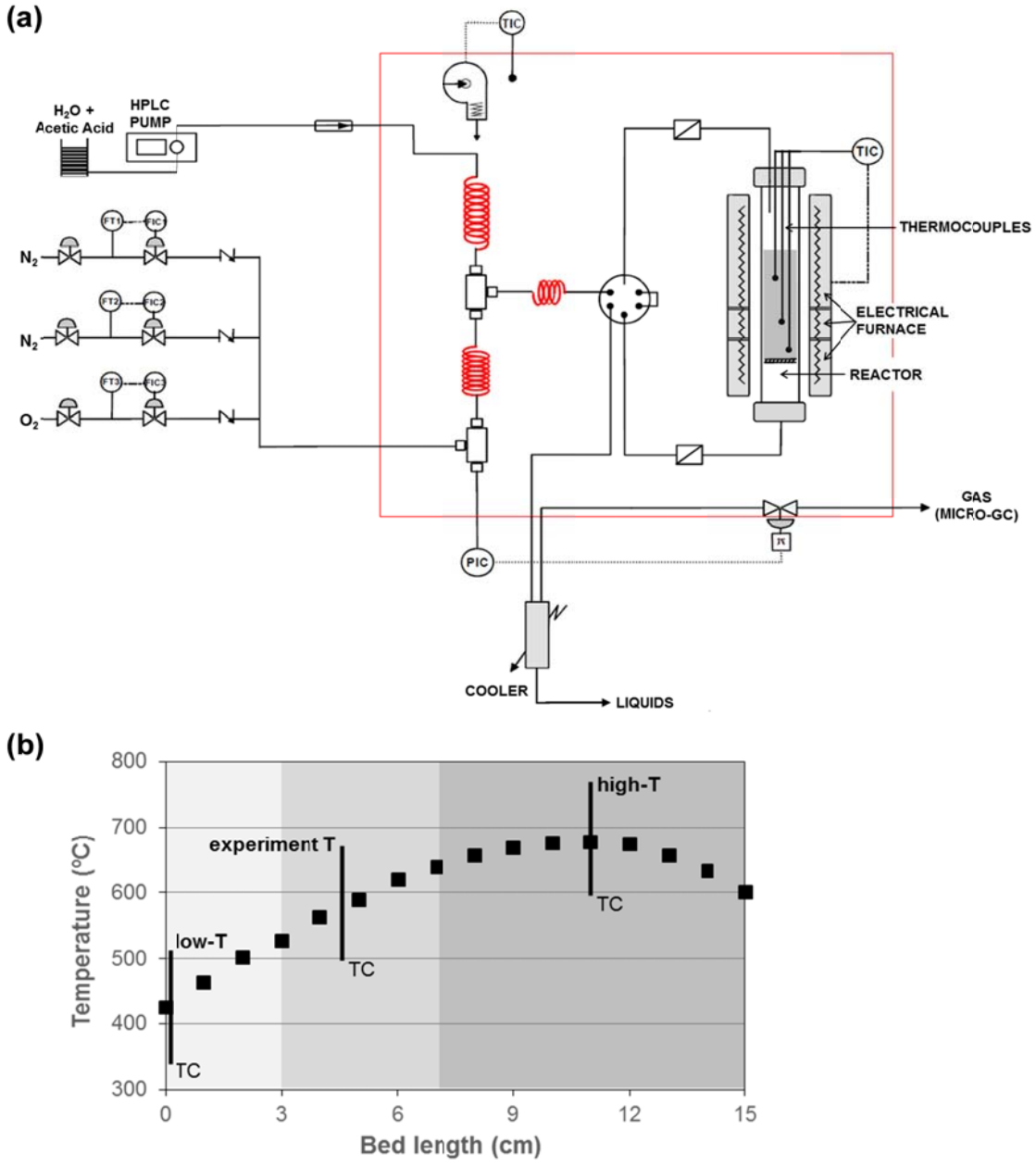

Fig. 1. (a) Schematic flow diagram of the experimental setup used for the SESR of acetic acid; (b) Temperature profile in the reactor (TC: thermocouple).

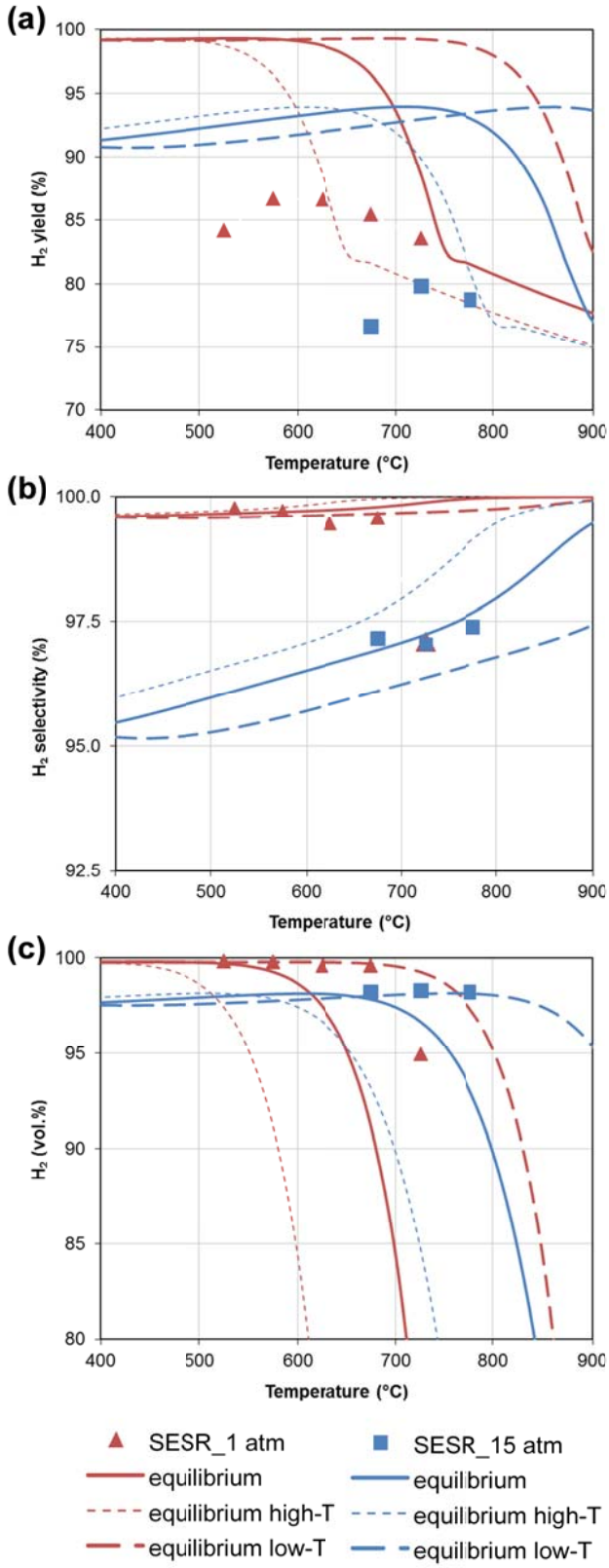

Fig. 2. Effect of the temperature and pressure on the H_2 yield (a), H_2 selectivity (b) and H_2 concentration (c) during the SESR of acetic acid. Reaction conditions: steam/C=3 mol/mol, WHSV=0.893 h^{-1}, sorbent/catalyst ratio=8 g/g, Pd/Ni-Co HT catalyst and dolomite as sorbent.

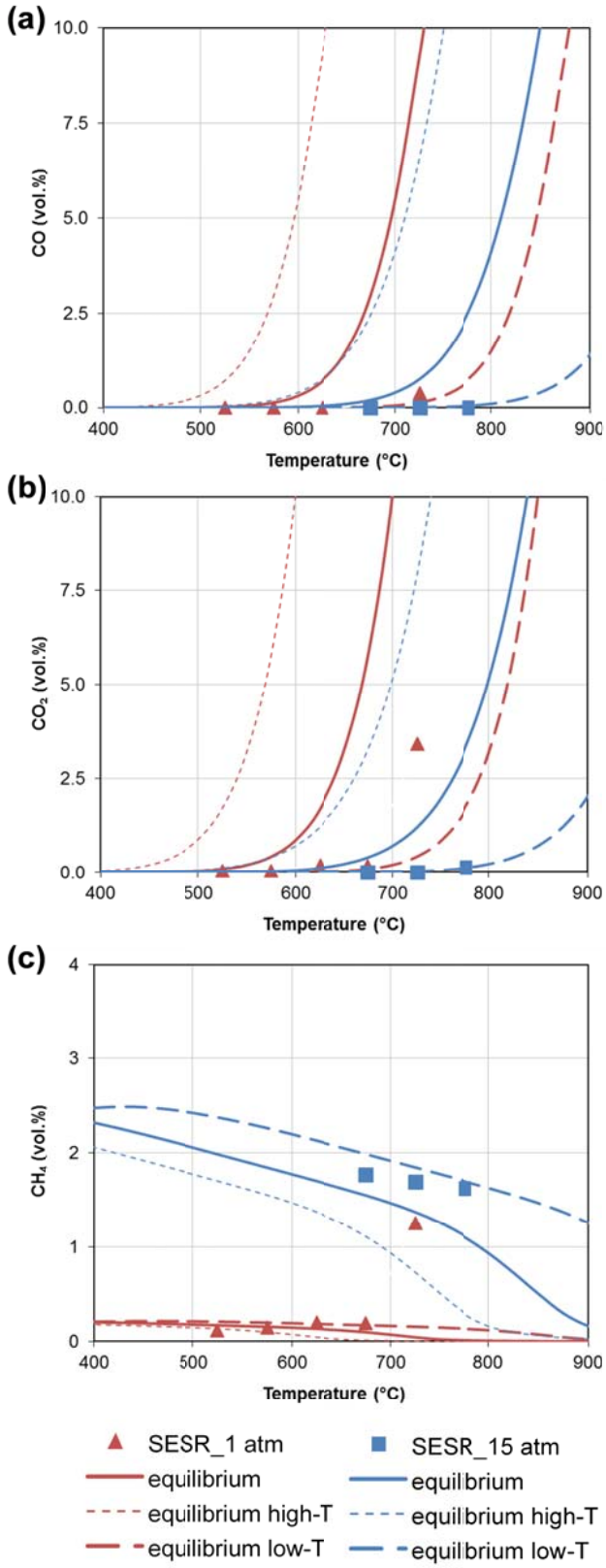

Fig. 3. Effect of the temperature and pressure on the CO (a), CO_2 (b) and CH_4 (c) concentrations during the SESR of acetic acid. Reaction conditions: steam/C=3 mol/mol, WHSV=0.893 h^{-1}, sorbent/catalyst ratio=8 g/g, Pd/Ni-Co HT catalyst and dolomite as sorbent.

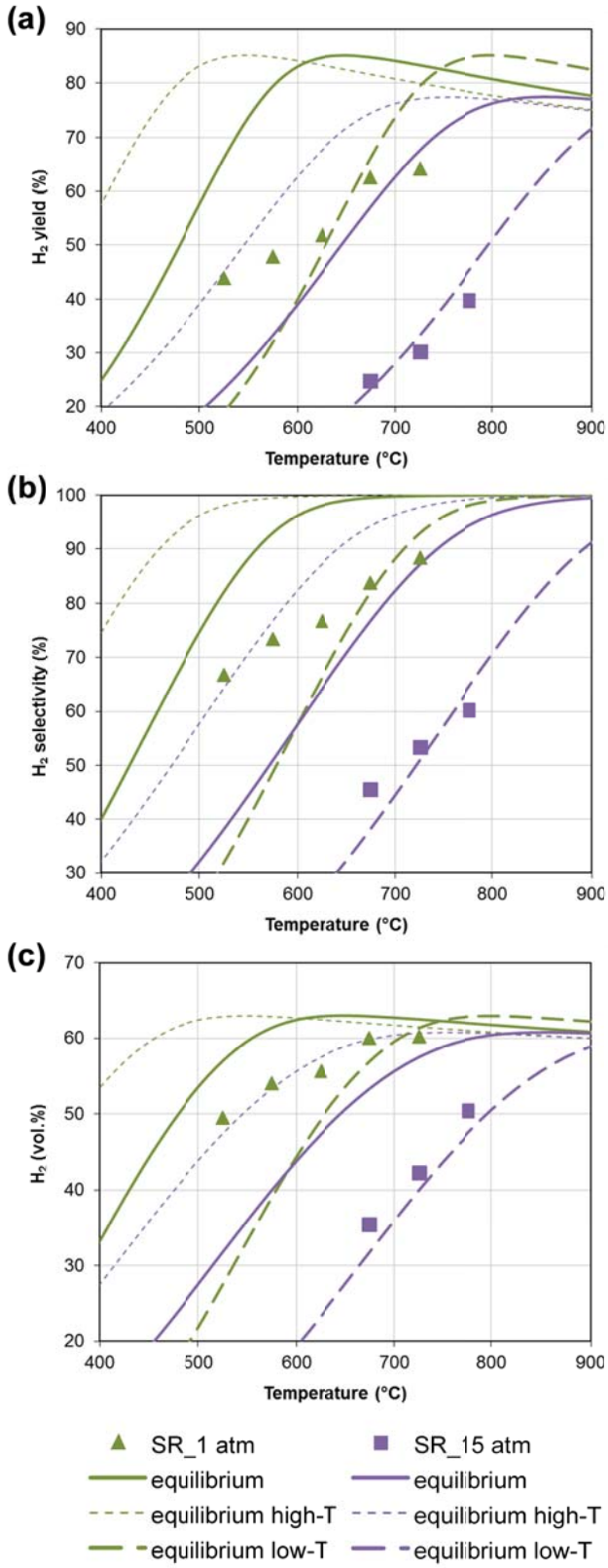

Fig. 4. Effect of the temperature and pressure on the H_2 yield (a), H_2 selectivity (b) and H_2 concentration (c) during the SR of acetic acid. Reaction conditions: steam/C=**3** mol/mol, WHSV=0.893 h^{-1}, sorbent/catalyst ratio=8 g/g, Pd/Ni-Co HT catalyst and dolomite as sorbent.

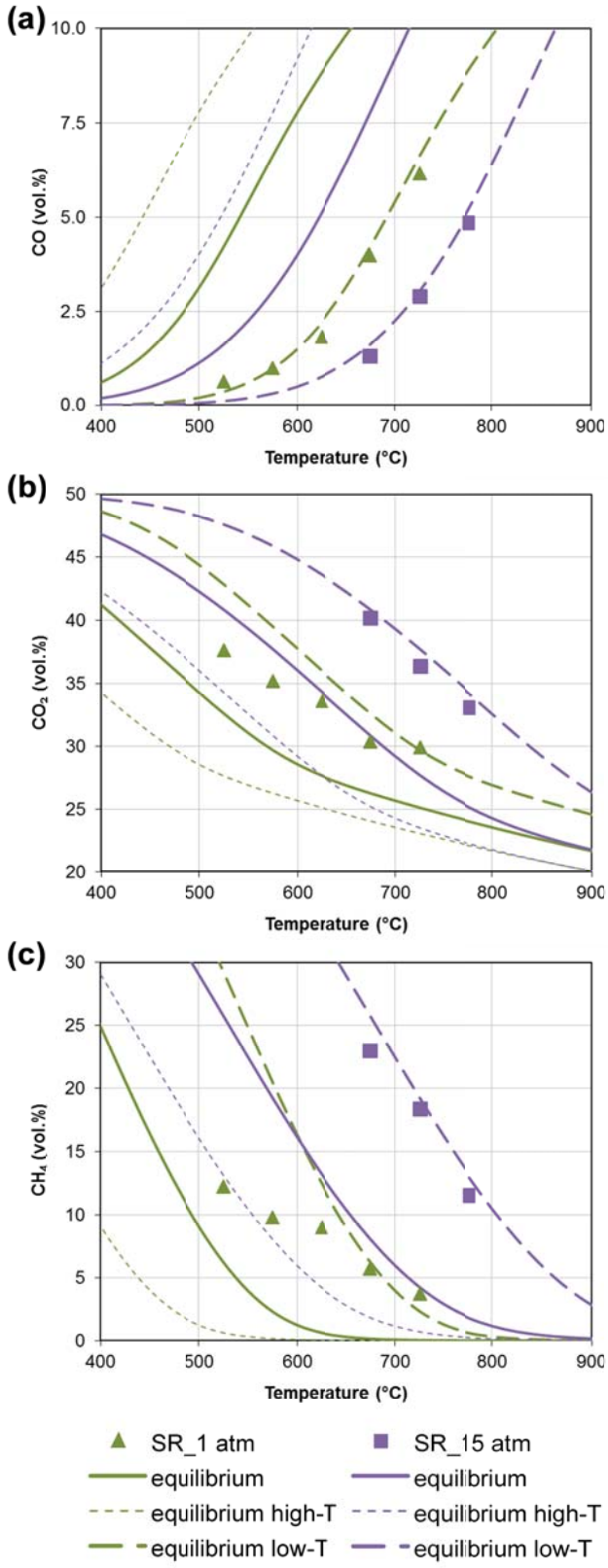

Fig. 5. Effect of the temperature and pressure on the CO (a), CO_2 (b) and CH_4 (c) concentrations during the SR of acetic acid. Reaction conditions: steam/C=3 mol/mol, WHSV=0.893 h^{-1}, sorbent/catalyst ratio=8 g/g, Pd/Ni-Co HT catalyst and dolomite as sorbent.

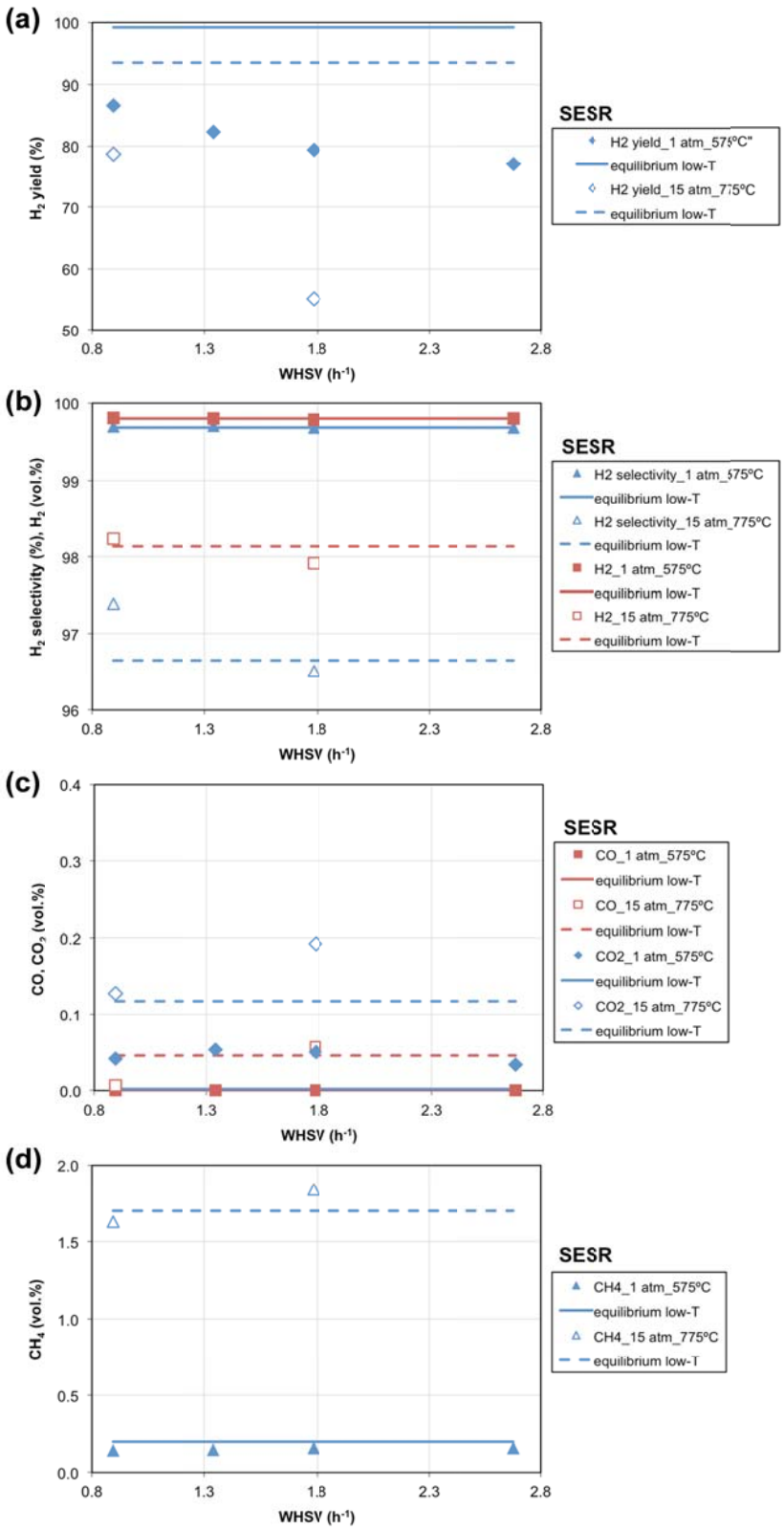

Fig. 6. Effect of the weight hourly space velocity (WHSV) and pressure on the H_2 yield (a), H_2 selectivity and H_2 concentration (b), CO and CO_2 concentrations (c) and CH_4 concentration (d) during the SESR of acetic acid. Reaction conditions: steam/C=3 mol/mol, sorbent/catalyst ratio=8 g/g, Pd/Ni-Co HT catalyst and dolomite as sorbent.

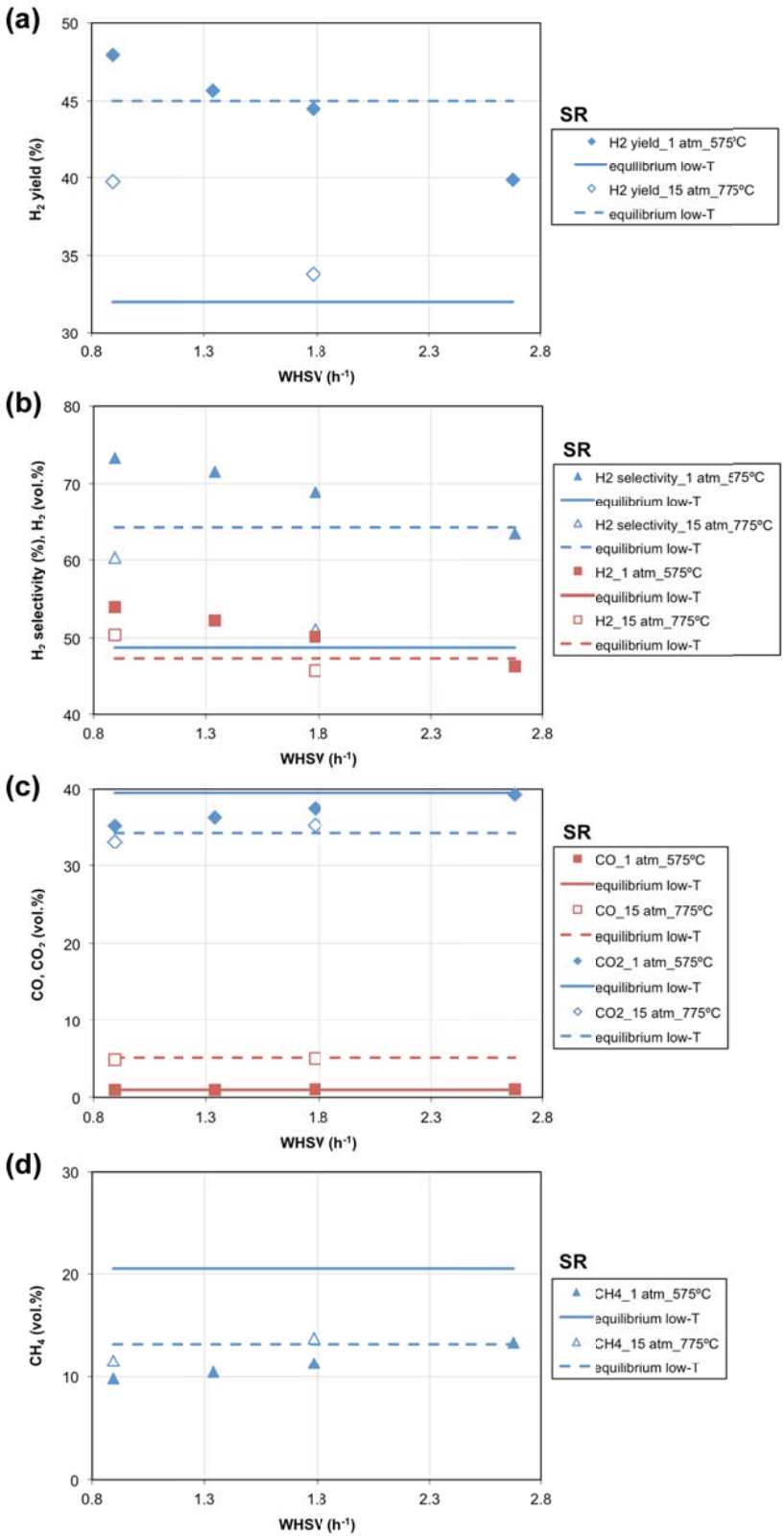

Fig. 7. Effect of the weight hourly space velocity (WHSV) and pressure on the H_2 yield (a), H_2 selectivity and H_2 concentration (b), CO and CO_2 concentrations (c) and CH_4 concentration (d) during the SR of acetic acid. Reaction conditions: steam/C=3 mol/mol, sorbent/catalyst ratio=8 g/g, Pd/Ni-Co HT catalyst and dolomite as sorbent.

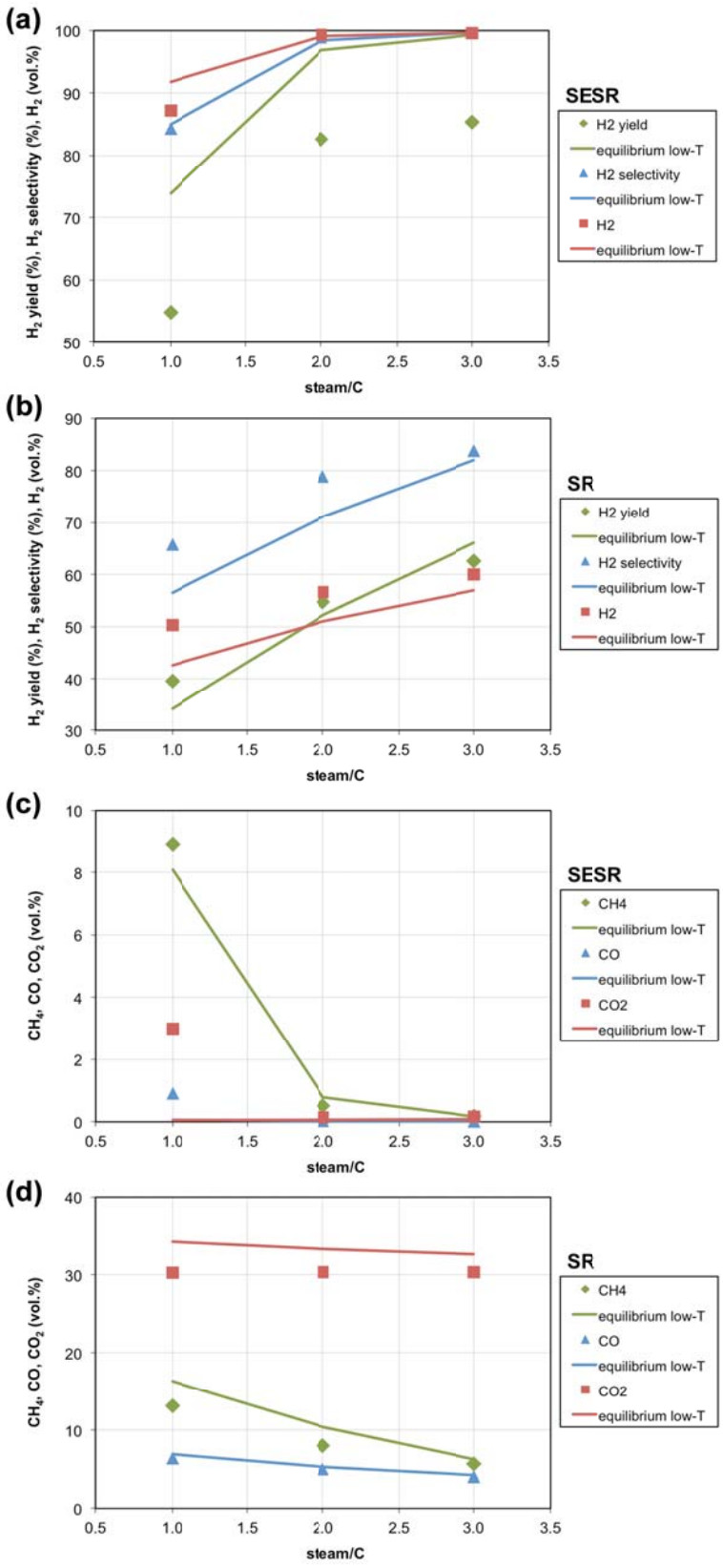

Fig. 8. Effect of the steam/C molar ratio on the SESR (a, c) and SR (b, d) of acetic acid. Reaction conditions: P=1 atm, T=675 ºC, WHSV=0.893-1.563 h^{-1}, sorbent/catalyst ratio=8 g/g, Pd/Ni-Co HT catalyst and dolomite as sorbent.